

## The Application of 2,6-Dichlorophenolindophenol-Functionalized Carbon nanotubes for Electrochemical Determination of Sulfide Ions

Alireza Mohadesi\*, Somayeh Parvaresh, Zarrin Eshaghi, Mohammad Ali Karimi

Department of Chemistry, Payame Noor University, P.O. Box 19395-3697 Tehran, Iran

Received: 14 August 2020

Accepted: 27 August 2020

DOI: 10.30473/ijac.2020.56689.1176

### Abstract

A chemically modified glassy carbon electrode was developed using multi-walled carbon nanotubes covalently immobilized with 2,6-dichlorophenolindophenol. The immobilization of 2,6-dichlorophenolindophenol with multi-walled carbon nanotubes was characterized by UV-visible absorption spectroscopy and Fourier transform infrared spectroscopy, and was determined using cyclic voltammetry. The cyclic voltammetric response of 2,6-dichlorophenolindophenol grafted onto multi-walled carbon nanotubes indicated that it promoted the electrocatalytic, sensitive and stable determination of sulfide ions. Meanwhile, the dependence of response currents on the concentration of sulfide was also examined and was linear in the range of 1.8  $\mu\text{M}$  – 2.5 mM. The detection limit of sulfide was 1.1  $\mu\text{M}$ , and RSD for 10 and 1000  $\mu\text{M}$  sulfide was 1.8 and 1.3 %, respectively. Many interfering species had little or no effect on the determination of sulfide. This procedure was applied for determination of sulfide in water samples.

### Keywords

2,6-Dichlorophenolindophenol; Sulfide; Carbon Nanotubes; Electrocatalysis; Functionalization.

### 1. INTRODUCTION

In aqueous solutions, hydrogen sulfide ( $\text{H}_2\text{S}$ ) is in equilibrium with bisulfide ( $\text{HS}^-$ ) and sulfide ions ( $\text{S}^{2-}$ ). Sulfides are widely found in natural water samples and wastewater and serve as a very important pollution index for water [1-2]. Several methods are available to measure sulfide in aqueous mediums. A comprehensive review on the analytical methods related to the detection of sulfide has been reported by Lawrence et al. [3]. The direct electrochemical oxidation of sulfide is highly irreversible with a great overpotential at the bare electrodes. In addition, the oxidized products of sulfide can be adsorbed on the electrode surface, which may result in the fouling and passivation of the electrode surface causing poor sensitivity, selectivity and also unstable analytical signals. The construction of chemically modified electrodes (CME) by the attachment of a catalytic species (organic or inorganic) to the surface of a base electrode is one of the treatment methods to solve these problems. Different approaches based on redox mediators including Cu(II)-alizarin complexone [4], ferricyanide [5-6], cobalt pentacyanonitrosylferrate [7], Cinder/tetracyano nikelate [8], hexadecylpyridinium-bis(chloranilato)-antimonyl(V) [9], 2,6-dichlorophenolindophenol [10], 2-(4-fluorophenyl)indolemodified xerogel [11], hemin functionalized reduced graphene oxide [12], Prussian Blue [13], hexadecachlorophthalocyanatoiron(II) [14], N,N'-Diphenyl-p-phenylenediamine [15], quercetin

[16], vanadium pentoxide [17-19], alizarin-reduced graphene oxide nanosheets [20], hematoxylin [21-22] and poly-methylene blue [23] have been utilized as voltammetric/ampereometric sensors to determine dissolved sulfide in the aqueous mediums.

One of the common methods which is very essential for the deposition of redox mediators and other species onto surfaces of carbon nanotubes (CNTs) is chemical modification which is used for nanocatalytic applications. As CNTs are large molecules with thousand atoms of carbon in an aromatic delocalized system, they are practically insoluble in all solvents, which results in their limited application. CNT, similar to graphite, is somewhat non-reactive, except at the caps of nanotube, which are more reactive because of the presence of dangling bonds. Accordingly, functionalization of CNTs is a compulsory task in order to increase the reactivity leading to wider application of CNTs. Currently, covalent and non-covalent functionalization of CNTs using organic compounds has become the subject of numerous studies to produce novel nanostructures with new functions and applications particularly for modification of electrode surfaces. Some of the previously reported functionalization approaches have included the origination of covalent bonds [24-26] while others have utilized noncovalent interactions [27-29] between modifier and CNT. In the present study, (i) 2,6-dichlorophenolindophenol (DPIP) as a redox

\*Corresponding Author: mohadesi\_a@yahoo.com

mediator was covalently attached to the multi-walled carbon nanotubes (MWNTs), (ii) a CME based on this nanomediator was prepared, and (iii) it was examined for electrocatalytic determination of sulfide in aqueous mediums.

## 2. EXPERIMENTAL

### 2.1. Materials

All reagents were of analytical reagent grade and were used without extra purification. DPIP was purchased from Merck, and MWNTs (95% purity) with an average outer diameter of 3-20 nm, length of 1-10  $\mu\text{m}$ , number of walls 3-15 and surface area of 350  $\text{m}^2 \text{g}^{-1}$ , were obtained from Palasmachem GmbH (Berlin, Germany). The stock solution of  $\text{Na}_2\text{S}$  (0.1 M) was prepared by dissolving  $\text{Na}_2\text{S}\cdot 9\text{H}_2\text{O}$  crystals in a degassed solution (0.1 M NaOH) and kept at  $+4^\circ\text{C}$ . This solution could be kept at most for a maximum of one week, and iodometric method was periodically used to standardize the solution. Phosphate buffer solution (PBS) with pH 7.5 which contained 0.1 M KCl was used as a supporting electrolyte for electrochemical studies. Deionized water was also used for all the experiments.

### 2.2. Apparatus

All voltammograms were recorded with a three-electrode system: 1) an Ag/AgCl as the reference electrode, 2) a platinum wire as the counter electrode, and 3) a glassy carbon electrode, GCE (3 mm diameter, Metrohm, Switzerland), modified with the following presented procedure, as the working electrode. The voltammetric experiments were performed using an Autolab electroanalyser Model PG-STAT-12 which was equipped with GPES software (version 4.9) running under Windows XP. To adjust pH, a Metrohm 710 pH meter was applied. The characterization of the functionalized-MWNTs was carried out using Jasco FT-IR 4200 spectrophotometer and also Cintra 6 GBC UV-Vis spectrophotometer. All the measurements were carried out at room temperature ( $22\pm 1^\circ\text{C}$ ).

### 2.3. Attaching the DPIP to the MWNTs

The raw MWNTs were first immersed in an aqueous HF solution to remove  $\text{SiO}_2$ ; then they were filtered and washed with distilled water. To remove the metals and amorphous carbon, they were refluxed in diluted  $\text{HNO}_3$  for 24 h. The obtained solid was then completely washed with deionized water and THF and dried in vacuum. It is well known that this procedure results in segmentation and production of  $-\text{COOH}$  groups at the terminus and sidewalls of MWNTs [30]. The COOH-MWNTs (100 mg) were suspended in an  $\text{SOCl}_2$  (25 ml) and DMF (1 ml) solution. The suspension was then stirred at  $65^\circ\text{C}$  for 24 h. After that, the solid was separated by filtration washed with anhydrous THF, and dried in vacuum. It is also obvious that these reactions cause conversion of  $-\text{COOH}$  groups at the terminus and sidewalls of MWNTs to  $-\text{COCl}$  groups. Later, these  $\text{COCl}$ -MWNTs (50 mg) were added to a solution of DPIP (100 mg) in degassed  $\text{CHCl}_3$  (10 ml), and the suspension was stirred for 20 h under  $\text{N}_2$  atmosphere at  $70^\circ\text{C}$ . Finally, the solid was separated by filtration, and washed exhaustively with THF and  $\text{CH}_2\text{Cl}_2$ , and dried in vacuum.

### 2.4. Preparation of modified electrode

First a  $0.6 \text{ mg mL}^{-1}$  DPIP-MWNT suspension was obtained by dispersing 6 mg of DPIP-MWNT in 10 mL of deionized water solution with the aid of ultrasonic agitation for 20 min. Before surface modification, a 3 mm glassy carbon electrode was polished with slurries of 0.05 mm alumina, and then it was cleaned ultrasonically in deionized water. The DPIP-MWNT film coated glassy carbon electrode (DPIP-MWNT/GCE) was prepared by casting a  $5 \mu\text{L}$  drop of the  $0.6 \text{ mg mL}^{-1}$  DPIP-MWNT suspension onto the well-polished GCE with a microsyringe. The solvent was then allowed to evaporate under room temperature. In a like procedure, the bare electrode was prepared without using unfunctionalized MWNTs.

### 2.5. Electrochemical studies

The electrochemical behavior of DPIP-MWNT/GCE was studied by recording the cyclic voltammograms in 0.1 M PBS (pH 7.5) including 0.1 M KCl at a scan rate of  $50 \text{ mV s}^{-1}$ . The effect of the scan rate on the peak potentials and peak currents was investigated by recording the cyclic voltammograms of the DPIP-MWNT/GCE at different scan rates in the potential range between  $-0.200$  and  $+0.250 \text{ V}$ . Moreover, the effect of pH between 4.5 and 9.5 on the peak potentials of the modified electrodes was also investigated at a scan rate of  $50 \text{ mV s}^{-1}$ . The electrocatalytic oxidation of sulfide at the DPIP-MWNT/GCE was investigated by cyclic voltammetry and hydrodynamic amperometry through the addition of a freshly prepared sulfide solution to the supporting electrolyte solution. The supporting electrolytes were deaerated by allowing highly pure nitrogen to pass through for 5 min before all the electrochemical experiments.

## 3. RESULT AND DISCUSSION

### 3.1. Characterization of MWNT functionalized with DPIP

With the aid of the previous procedure, the functionalization of MWNTs with DPIP was carried out [31]. The reaction scheme is shown in Fig. 1.

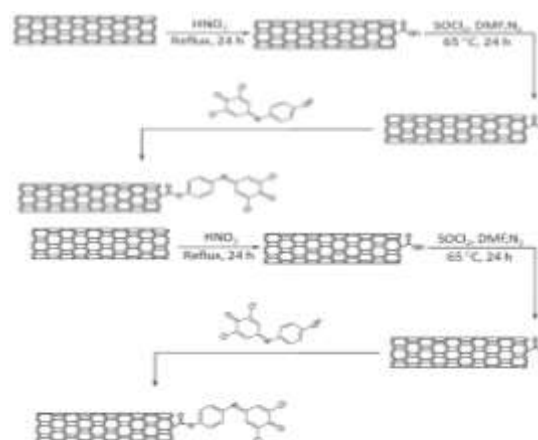
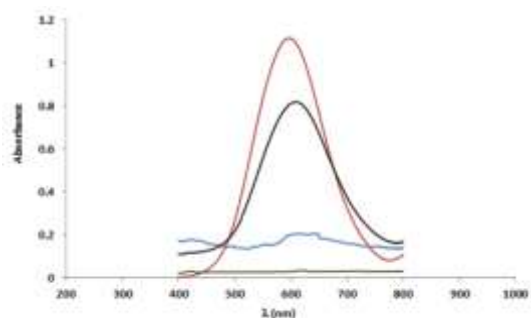


Fig. 1 Anchoring the DPIP to the MWNTs

To investigate the interactions between MWNT and DPIP, UV-visible absorption measurements were used. The UV-visible absorption spectra of

DPIP and DPIP-MWNT suspended solutions are shown in Fig. 2a and b, respectively. It was discovered that the UV-visible spectrum of the pure DPIP had one distinctive absorption peak in visible region around 592 nm. Moreover, observing this peak in DPIP modified MWNTs solution indicated the existence of DPIP molecules on MWNTs. The clear red shift for this peak also provided additional verifications for the immobilization of DPIP with MWNTs. These observations are in good accordance with the earlier reports [30-31].



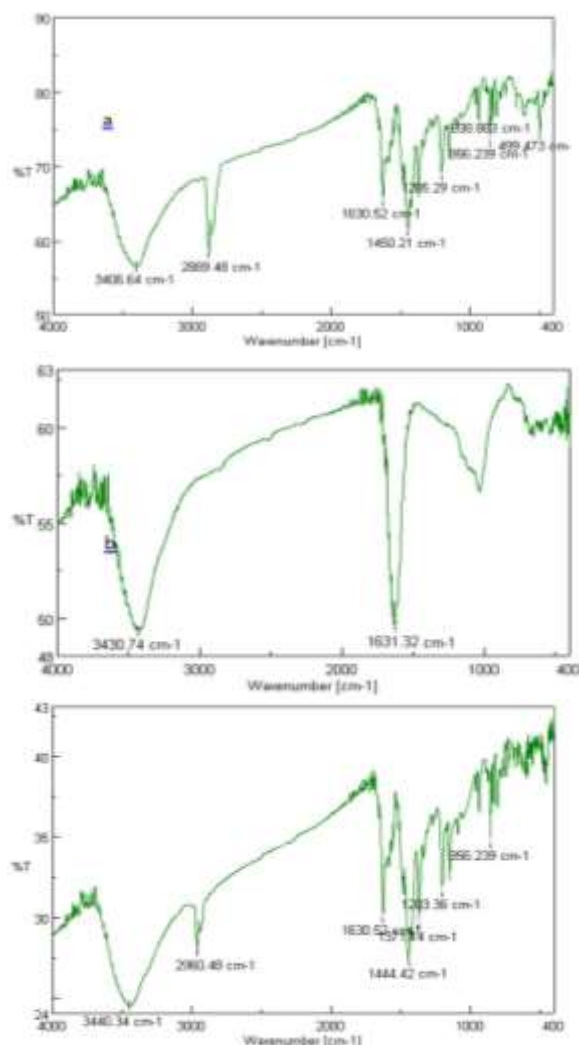
**Fig. 2** UV-visible absorption spectra of (a) DPIP in aqueous solution, (b) DPIP-MWNT suspended solution, (c) MWNT suspended solution and (d) deionized water.

Fig. 3a, b and c show the Fourier-transformed infrared spectra of as DPIP, carboxylated MWNTs and DPIP functionalized MWNTs, respectively. The COOH-MWNTs yielded three major peaks at wave numbers near 1400, 1700 and 3500  $\text{cm}^{-1}$ , which were related to aromatic  $-\text{C}=\text{C}$  groups, carbonyl groups ( $-\text{C}=\text{O}$ ) from carboxylic acids ( $-\text{COOH}$ ), and alcoholic groups ( $-\text{COH}$ ) or hydroxyl groups ( $-\text{OH}$ ) from carboxylic acids [30,32], respectively. Meanwhile, the FT-IR spectra of DPIP-MWNT performed similar bands under 1600  $\text{cm}^{-1}$  and also a band at 2900  $\text{cm}^{-1}$  when MWNTs were functionalized with DPIP. These bands were also exhibited with DPIP [33] which looked like those in the presence of DPIP modified onto MWNT surface.

### 3.2. Electrochemical behavior of modified electrode

Cyclic voltammetric tests were performed to investigate the electrochemical behavior of the DPIP-MWNT/GCE. The cyclic voltammograms (CVs) are shown in Fig. 4. The figure shows the electrochemical behaviors of bare GCE (curve a), MWNT/GCE (curve b) and DPIP-MWNT/GCE (curve c) in a 0.1 M phosphate buffer solution (pH 7.5). As seen, the bare GCE basically displayed no voltammetric reactions in the studied potential range while a pair of unclear and

negligible redox peaks were noticed for MWNT/GCE. These peaks were stable over reiterative cycling and were associated with the existence of oxygen containing functional groups in the oxidized sample of MWNT.



**Fig. 3.** The Fourier-transformed infrared spectra of as (a) DPIP, (b) carboxylated MWNTs and (c) DPIP functionalized MWNTs.

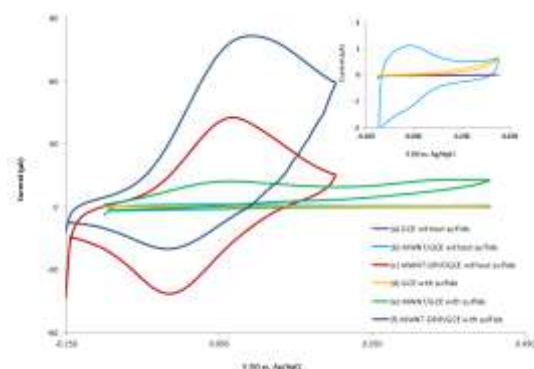


**Fig. 4** The CVs (50 mV/s) in a 0.1 M PBS with pH=7.5 for (a) bare GCE, (b) MWNT/GCE, (c) DPIP-MWNT/GCE, (d-f) a-c with 5 mM sulfide in solution.

During acid purification of MWNT, these functional groups were created specially at surface handicaps (e.g., open ends of carbon nanotubes). Certainly, the presence of surface handicaps was responsible for electron transfer and chemical reactivity of carbon nanotubes. The catalytic active surface of nanotubes caused the large background current [30, 32]. MWNTs had very high aspect ratio because of the diameters in the range of 10–20 nm, and up to several microns in length have very high aspect ratio (length versus diameter). Therefore, the surface area of the electrode was large. Thus, the background current at the MWNT immobilized electrode was greater than that at the bare surface. DPIP-MWNT/GCE showed a couple of reversible reduction and oxidation peaks with cathodic and anodic peak potentials at -0.014 and +0.066 V (vs. Ag/AgCl), respectively. The appearances of the anodic and cathodic peaks were closely symmetrical, and the reduction and oxidation peaks had equal heights ( $\Delta E_p=80$  mV value proposes that DPIP undergoes a quasi-reversible redox reaction at the electrode).

To confirm the association between current response and surface confined DPIP molecules, we performed a study to check the dependence of the peak currents on the scan rate. Fig. 5A displays the CVs of DPIP-MWNT/GCE obtained at 9 different scan rates. It was observed that the peak current increased linearly with increasing scan rate, while  $\Delta E_p$  also increases. The  $I_{pc}$  and  $I_{pa}$  vs.  $v$  plot shown in Fig. 5B display linear correlations representing that the redox reaction was a surface confined process. Consequently, DPIP immobilized onto the surface of MWNTs underwent electron transfer reactions. Since the surfaces of MWNTs were recognized to improve many electrochemical reactions, the easy electron transfer reaction happened.

Furthermore, increasing the scan rates, the reduction peak shifted to more negative potentials although the oxidation peak shifted to more positive potentials. Through the theory of Laviron [341], the anodic and cathodic peak potentials were linearly dependent on the logarithm of scan rates when  $\Delta E_p > 200/n$ . A plot of  $E_p$  versus  $\log v$  (Fig. 5C) provided two straight lines with slope of  $-2.3RT/\alpha nF$  for the cathodic peak and  $2.3RT/(1 - \alpha)nF$  for the anodic peak so that  $\alpha$  could be evaluated as 0.55 from the slope of the straight lines based on the following equation:

$$\frac{v_a}{v_c} = \frac{\alpha}{1-\alpha} \quad (1)$$

The rate constant of electron transfer ( $k_s$ ) was evaluated to be  $1.61 \text{ s}^{-1}$  according to the equation:

$$k_s = \frac{\alpha n F v_c}{RT} = \frac{(1-\alpha)n F v_a}{RT} \quad (2)$$

The surface concentration of electroactive species could be estimated from the slope of the plot of peak currents versus scan rate. By the Sharp equation [34], the peak current was related to the surface concentration of electroactive species:

$$I_p = \frac{n^2 F^2 A \Gamma v}{4RT} \quad (3)$$

where  $n$  depicts the number of electrons involved in reaction (two for DPIP),  $A$  the surface geometrical area ( $0.07065 \text{ cm}^2$ ),  $\Gamma$  ( $\text{mol cm}^{-2}$ ) the surface coverage and other symbols have their normal meaning. The surface concentration of DPIP was calculated  $2.7 \times 10^{-9} \text{ mol cm}^{-2}$  from the slope of anodic peak currents versus scan rate (Fig. 5B).

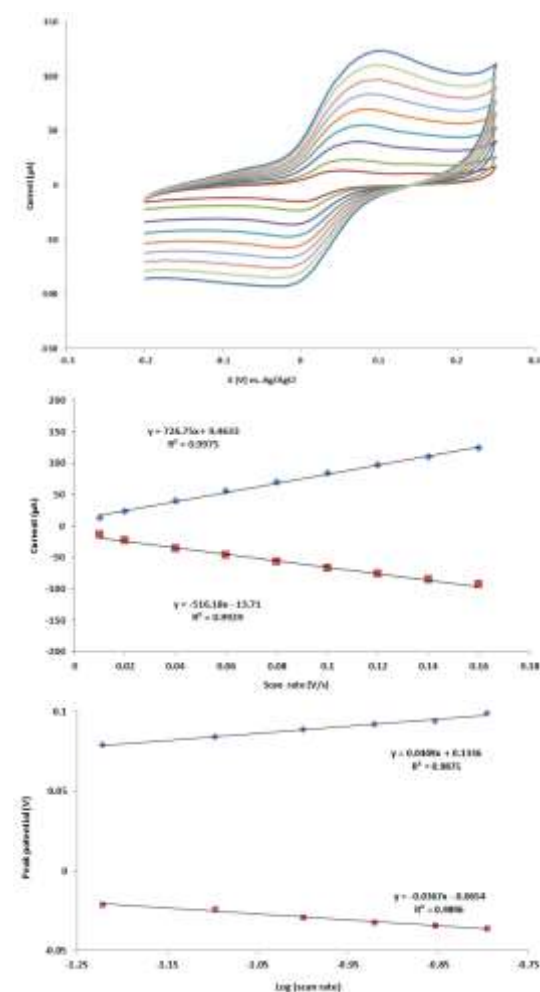


**Fig. 5** The CVs of the DPIP-MWNT/GCE in 0.1 M PBS with pH=7.5 at different scan rates (a-i): 10-160 mV/s (A). Plots of anodic and cathodic peak currents vs. potential scan rates (B). Plots of anodic and cathodic peak potentials vs. logarithm of scan rates (C).

To confirm the effect of pH on the peak potentials of the modified electrodes, the cyclic voltammograms of DPIP-MWNT were recorded in buffer solutions containing 0.1 M KCl of pH values between 4.5 and 9.5 at a scan rate of 50

$\text{mV s}^{-1}$ . Cathodic and anodic peak potentials of DPIP are shifted to less positive potentials when the pH increased (curves a Fig.6A). As shown in (Fig. 6B), the relevance between pH and anodic peak potential of DPIP was linear with a slope of  $-67.9 \text{ mV}$  per unit of pH which was very close to the predicted Nernstian value of  $-59 \text{ mV}$ . Consequently, it was observed that the number of transferred electrons and protons was equal in the DPIP electrochemical reaction. Our results were also in agreement with other achievements, in which the number of electrons and protons was found to be 2 for DPIP oxidation at different electrodes [10, 35].

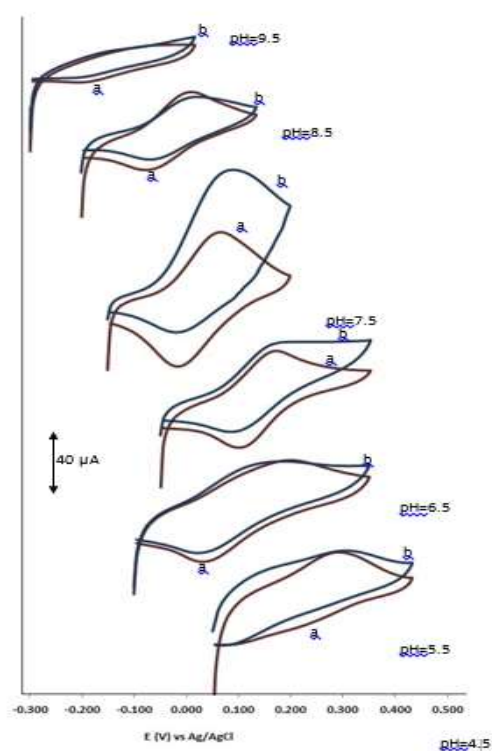


**Fig. 6** The CVs of the DPIP-MWNT/GCE in 0.1 M phosphate solutions containing 0.1 M KCl at different pHs. Curves (a) are without sulfide ions and curves (b) are with 5 mM sulfide ions in solutions.

### 3.3. Sulfide electrocatalytic determination at DPIP-MWNT/GCE

In the presence of sulfide at a DPIP-MWNT/GCE, the anodic peak of DPIP significantly increased with a decrease in the cathodic peak current (curve f Fig.4). This showed that the oxidation reaction of sulfide happened on the MWNT surface through DPIP as a mediator. Thus, under the same experimental conditions, an unfunctionalized MWNT/GCE

(curve e) and bare GCE (curve d) were subjected for the oxidation of sulfide. Direct sulfide oxidation on these electrodes occurred in more positive potentials and also with lower anodic currents. Consequently, mediated sulfide oxidation on the DPIP-MWNT surface could provide a better sensitivity but also avoid the interference of other easily oxidizable compounds.

Furthermore, the effect of pH on the DPIP-MWNT/GCE electrocatalytic behavior was studied. As shown in Fig. 6A (curves b), the best shape and highest electrocatalytic current was observed at  $\text{pH}=7.5$ .

Then, hydrodynamic amperometry at the DPIP-MWNT/GCE was studied for sulfide determination. Under a detection potential of 0.100 V in pH 7.5 of PBS and, a linear calibration in the range of 1.8  $\mu\text{M}$  up to 2.5 mM was acquired with a current sensitivity of 52  $\mu\text{A}/\text{mM}$  and regression of 0.995. By continuous eight additions of 10 and 1000  $\mu\text{M}$  sulfide, RSDs were obtained of 1.8 and 1.3 %, respectively. Using the equation  $\text{LOD} = 3s_b/m$ , the detection limit (D.L.) was found to be 1.1  $\mu\text{M}$  sulfide where  $s_b$  is the standard deviation of the blank response and m is the calibration plot slope.

### 3.4. Chronoamperometric and RDE voltammetric studies

The sulfide diffusion coefficient was calculated by the catalytic oxidation of sulfide through the DPIP-MWNT/GCE using chronoamperometric method. As shown in Fig.7A, the chronoamperograms demonstrated that an increase in anodic peak current achieved for a potential step of 0.100 V. The diffusion coefficient, D, was described through the Cottrell equation when the oxidation current for the electrochemical reaction of an electroactive material was controlled under mass transfer.

$$I = \frac{nFAD^{1/2}C^*}{\pi^{1/2}t^{1/2}} \quad (4)$$

The plot of I against  $t^{-1/2}$  would be linear, and from the plot slope value, the diffusion coefficient, D, could be calculated. Fig. 7B shows the experimental plots with different sulfide concentrations. Then the resulting straight line slopes were plotted versus the sulfide concentrations (Fig. 7C). So, the diffusion coefficient was calculated as  $1.06 \times 10^{-5} \text{ cm}^2 \text{ s}^{-1}$  from the slope of this straight line.

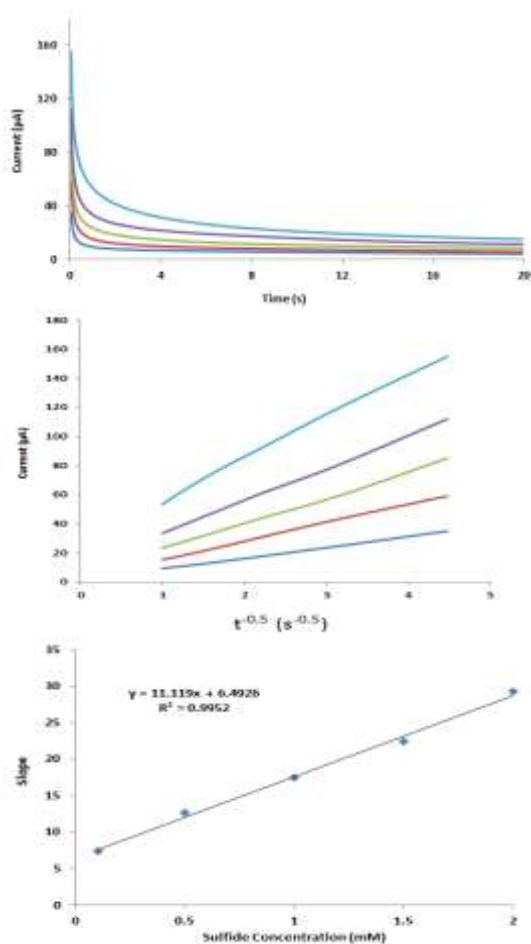


**Fig. 7** (A) Chronoamperometric responses of DPIP-MWNT/GCE in 0.1 M PBS (pH 7.5) at potential step of 100 mV for different concentrations of sulfide. The curves (a)-(e) correspond to 0.1, 0.5, 1.0, 1.5 and 2.0 mM sulfide. (B) Plots of current vs.  $t^{-1/2}$  obtained from the chronoamperograms shown in (A). (C) Plot of the slopes of the straight lines shown in (B) against the sulfide concentration.

In addition, RDE voltammetry was used to evaluate the electrocatalytic activity of DPIP-MWNT/GCE for sulfide oxidation. The steady-state I-E curves were recorded for the sulfide oxidation. Fig. 8A shows the RDE voltammograms at rotation speed range 300 - 1750 rpm for 1.0 mM sulfide. If the sulfide oxidation at the DPIP-MWNT/GCE is just controlled by the process of mass transfer in the solution, the relevance between the limiting current and rotating speed should obtain by the Levich equation [34]:

$$I_{Lev} = 0.62nFAD^{2/3}\gamma^{-1/6}\omega^{1/2}C^* \quad (5)$$

where  $D$  is the diffusion coefficient,  $\gamma$  is the kinematic viscosity,  $\omega$  is the RDE rotation speed and  $C^*$  is the bulk concentration of the reactant (sulfide) in the solution. All other symbols have their usual meanings. According to Eq. (5), the plot of limiting current  $I_{Lev}$  as function of the  $\omega^{1/2}$

should be a straight line. As shown in Fig. 8B, through the Levich plot, at 0.100 V, the current increased with the increasing rotation speed of the electrode. For the reason that, the oxidation rate of the DPIP at the electrode and the mass transport of sulfide from bulk solution to the surface of electrode at 0.100 V, can be fast, this would propose that the sulfide catalytic oxidation is the rate-determining step. Therefore, to calculate the reaction rate constant ( $k_c$ ) between combined DPIP and sulfide, the Koutecky-Levich equation (Eq. 6) can be applied:

$$[I_{Lev}]^{-1} = [nFACk_c\Gamma]^{-1} + [0.62nFAD^{2/3}\gamma^{-1/6}\omega^{1/2}C^*]^{-1} \quad (6)$$

The plot of Koutecky-Levich is shown in Fig. 8C obtained from the data in Fig. 8B. This plot shows the predicted linear relevance between  $I^{-1}$  and  $\omega^{1/2}$ . From the intercept of plot in Fig. 8C, the rate constant,  $k_c$ , was found to be  $1.75 \times 10^6 \text{ cm}^3 \text{ mol}^{-1} \text{ s}^{-1}$ .

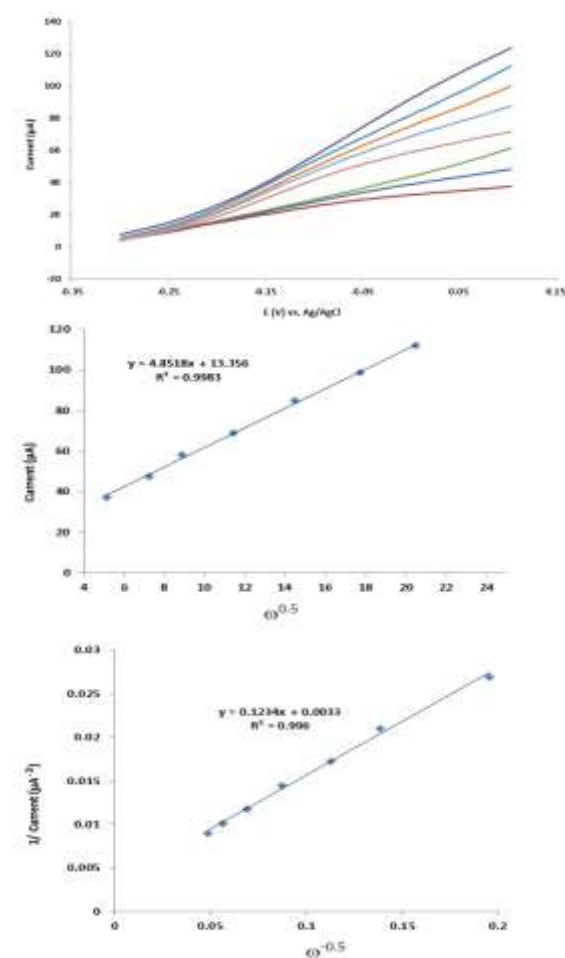


**Fig. 8** (A) RDE voltammograms for the oxidation of 1.0 mM sulfide at the DPIP-MWNT/GCE in 0.1 M PBS (pH 7.5). The rotation speeds from (a) to (h) are 250, 500, 750, 1250, 2000, 3000, 4000 and 5000 rpm, respectively, with a scan rate of  $5 \text{ mVs}^{-1}$ . (B) shows the Levich plot for catalytic oxidation of sulfide at 0.1 V. (C) Koutecky-Levich plot for 1.0 mM sulfide at the DPIP-MWNT/GCE at oxidation potential of 0.1 V.

### 3.5. Interference and real sample studies

The influence of various species interference and common components of environmental matrix on the signal of sulfide was analyzed in the presence of 0.2 mM Na<sub>2</sub>S. For metal cations, 2 mM solutions of the relevant salts of nitrate or chloride were analyzed without sulfide because it is declared that metal ions compose insoluble sulfides. The response for Mn<sup>2+</sup>, Zn<sup>2+</sup>, Mg<sup>2+</sup>, Co<sup>2+</sup>, Pb<sup>2+</sup>, Na<sup>+</sup>, Ca<sup>2+</sup>, Fe<sup>3+</sup>, Fe<sup>2+</sup> and Cu<sup>2+</sup> was not detectable. For anions, 2 mM solutions of the relevant sodium or potassium salts were analyzed with sulfide. In the presence of SO<sub>3</sub><sup>2-</sup>, SO<sub>4</sub><sup>2-</sup>, S<sub>2</sub>O<sub>3</sub><sup>2-</sup>, SCN<sup>-</sup>, NO<sub>3</sub><sup>-</sup>, NO<sub>2</sub><sup>-</sup>, CO<sub>3</sub><sup>2-</sup>, I<sup>-</sup>, Cl<sup>-</sup> and F<sup>-</sup>, no interference effect was noticed. Additionally, no effect of interference was observed in the presence of uric acid, dopamine, acetaminophen and epinephrine. Just ascorbic acid and cysteine demonstrated serious positive interference with recoveries of 182 and 149 %, respectively. But their interferences can be ignored, because these compounds are rarely present in real sulfide samples. The following system for practical application was used to determine the sulfide content in ground and waste waters. It was carried out by spiking known amounts of sulfide in these real samples, without any sulfides, and their results for various matrices are resumed in Table 1. These conclusions confirm the practical application of the present procedure in sensor application.

**Table 1.** Determination of sulphide in water samples.

Sample	Added sulfide (μM)	Taken sulfide (μM) <sup>a</sup>	Recoveries (%)
Waste water	0	No detect	-
	10.0	10.1 ± 0.2	101.0
	1000.0	1014.9 ± 19.4	101.5
Ground water	0	No detect	-
	10.0	10.3 ± 0.1	103.0
	1000.0	1016.8 ± 17.3	101.7

<sup>a</sup> Average of three runs ± standard deviation

## 4. CONCLUSION

The MWNTs covalently bonded by DPIP were successfully achieved by the chemical modification methods. This functionalized MWNT was utilized to modify the surface of glassy carbon electrode, and its electrochemical behavior was examined in aqueous solutions. This modified electrode was tested for electrocatalytic sulfide determination in aqueous medium.

## REFERENCES

- [1] A. Baciú, M. Ardelean, A. Pop, R. Pode, and F. Manea, Simultaneous Voltammetric/Amperometric Determination of Sulfide and Nitrite in Water at BDD Electrode, *Sensors* (2015) 14526-14538.
- [2] F. Liu, Y. Gao, W. Li, J. Shao and Y. Meng, Determination of sodium sulfide based on electrochemiluminescence of rhodamine B at a SWNT modified glassy carbon electrode, *RSC Adv* (2014) 16893–16898.
- [3] N.S. Lawrence, J. Davis and R.G. Compton, Analytical strategies for the detection of sulfide: a review, *Talanta* (2000) 771–784.
- [4] J. Zhang, A.B.P. Lever and W.J. Pietro, Surface copper immobilization by chelation of alizarin complexone and electrodeposition on graphite electrodes, and related hydrogen sulfide electrochemistry; matrix isolation of atomic copper and molecular copper sulfides on a graphite electrode, *J. Electroanal. Chem.* (1995) 191-200.
- [5] D.M. Tsai, A.S. Kumar and J.M. Zen, A highly stable and sensitive chemically modified screen-printed electrode for sulfide analysis, *Anal. Chim. Acta* (2006) 145–150.
- [6] J.L. Chang, G.T. Wei, T. Chen and J. Zen, Highly Stable Polymeric Ionic Liquid Modified Electrode to Immobilize Ferricyanide for Electroanalysis of Sulfide, *Electroanalysis* (2013) 845–849.
- [7] L.L. Paim and N.R. Stradiotto, Electrooxidation of sulfide by cobalt pentacyanonitrosylferrate film on glassy carbon electrode by cyclic voltammetry, *Electrochim Acta* (2010) 4144–4147.
- [8] J.M. Zen, J.L. Chang, P.Y. Chen, R. Ohara and K.C. Pan, Flow injection analysis of sulfide using a cinder/tetracyano nikelate modified screen-printed electrode, *Electroanalysis* (2005) 739–743.
- [9] M.I. Prodromidis, P.G. Veltsistas, M.I. Karayannis, Electrochemical study of chemically modified and screen-printed graphite electrodes with [(SbO)–O–V(CHL)(2)]Hex. Application for the selective determination of sulfide, *Anal. Chem.* (2000) 3995–4002.
- [10] A.B. Florou, M.I. Prodromidis, M.I. Karayannis and S.M. Tzouwara-Karayanni, Electrocatalysis of sulphide with a cellulose acetate film bearing 2,6-dichlorophenolindophenol. Application to sewage using a fully automated flow injection manifold *Talanta* (2000) 465–472.
- [11] G. Roman, A.C. Pappas, D.K. Demertzi and M.I. Prodromidis, Preparation of a 2-(4-fluorophenyl)indole-modified xerogel and its

- use for the fabrication of screenprinted electrodes for the electrocatalytic determination of sulfide. *Anal Chim Acta* (2004) 201–207.
- [12] X. Cao, J. Gao, Y. Ye, P. Wang, S. Ding, Y. Ye and H. Sun, Amperometric Determination of Sulfide by Glassy Carbon Electrode Modified with Hemin Functionalized Reduced Graphene Oxide. *Electroanalysis* (2016) 140–144.
- [13] B. Eetek, D. Long Vu, L.C. Ervenka and Y. Dilgin, Flow Injection Amperometric Detection of Sulfide Using a Prussian Blue Modified Glassy Carbon Electrode. *Anal. Sci.* (2012) 1075–1080.
- [14] J. Zhang, A.B.P. Lever and W.J. Pietro, Electrocatalytic activity of a graphite electrode coated with hexadecachloro phthalocyanatoiron(II) toward sulfide oxidation, and its possible application in electroanalysis. *Can. J. Chem.* (1995) 1072–1077.
- [15] N.S. Lawrence, L. Jiang, T.G.J. Jones and R.G. Compton, Voltammetric Characterization of a N,N-Diphenyl-p-phenylene diamine-Loaded Screen-Printed Electrode: A Disposable Sensor for Hydrogen Sulfide. *Anal. Chem.* (2003) 2054–2059.
- [16] Y. Dilgin, B. Kızılkaya, B. Ertek, N. Eren and D.G. Dilgin, Amperometric determination of sulfide based on its electrocatalytic oxidation at a pencil graphite electrode modified with quercetin. *Talanta* (2012) 490–495.
- [17] E.A. Khudaish, Mass and electron-transfer conditions for the electrochemical oxidation of hydrogen sulfide at vanadium pentoxide film modified electrode. *Sensor Actuat B-Chem* (2008) 223–229.
- [18] E.A. Khudaish and A.T. Al-Hinai, The catalytic activity of vanadium pentoxide film modified electrode on the electrochemical oxidation of hydrogen sulfide in alkaline solutions. *J. Electroanal. Chem.* (2006) 108–114.
- [19] J.A. Bennett, J.E. Pander and M.A. Neiswonger, Investigating the viability of electrodeposited vanadium pentoxide as a suitable electrode material for in vivo amperometric hydrogen sulfide detection. *J. Electroanal Chem.* (2001) 1–7.
- [20] X. Cao, H. Xu, S. Ding, Y. Ye, X. Ge and L. Yu, Electrochemical determination of sulfide in fruits using alizarin-reduced graphene oxide nanosheets modified electrode. *Food Chem.* (2016) 1224–1229.
- [21] Y. Dilgin, B. Kızılkaya, B. Ertek, F. Is and D. Giray Dilgin, Electrocatalytic oxidation of sulphide using a pencil graphite electrode modified with hematoxylin. *Sensor Actuat B-Chem.* (2012) 223–229.
- [22] D.L. Vu and L. Cervenka, Determination of Sulfide by Hematoxylin Multiwalled Carbon Nanotubes Modified Carbon Paste Electrode. *Electroanalysis* (2013) 1967–1973.
- [23] Y. Dilgin, S. Canarlan, O. Ayyildiz, B. Ertek and G. Nisli, Flow injection analysis of sulphide based on its photoelectrocatalytic oxidation at poly-methylene blue modified glassy carbon electrode. *Electrochim Acta* (2012) 173–179.
- [24] R. Zhang, X. Wang and K.K. Shiu, Accelerated direct electrochemistry of hemoglobin based on hemoglobin-carbon nanotube (Hb-CNT) assembly. *J. Colloid. Interface. Sci.* (2007) 517–522.
- [25] Y. Liu, Y. Li, Z.Q. Wu and X. Yan, Fabrication and characterization of hexahistidine-tagged protein functionalized multi-walled carbon nanotubes for selective solid-phase extraction of Cu<sup>2+</sup> and Ni<sup>2+</sup>. *Talanta* (2009) 1464–1471.
- [26] L. Li, Y. Huang, Y. Wang and W. Wang, Hemimicelle capped functionalized carbon nanotubes-based nanosized solid-phase extraction of arsenic from environmental water samples. *Anal. Chim. Acta* (2009) 182–188.
- [27] A. Mohadesi, Z. Motallebi and A. Salmanipour, Multiwalled carbon nanotube modified with 1-(2-pyridylazo)-2-naphthol for stripping voltammetric determination of Pb(II). *Analyst* (2010) 1686–1690.
- [28] A. Mohadesi, H. Beitollahi and M.A. Karimi, Stripping voltammetric determination of Cd(II) based on multiwalled carbon nanotube functionalized with 1-(2-pyridylazo)-2-naphthol. *Chin. Chem. Lett.* (2011) 1469–1472.
- [29] A. Salmanipour and M.A. Taher, An electrochemical sensor for stripping analysis of Pb(II) based on multiwalled carbon nanotube functionalized with 5-Br-PADAP. *J. Solid State Electrochem.* (2011) 2695–2702.
- [30] D.R. Shobha, A. Jeykumari, S. Ramaprabhu and S.S. Narayanan, A thionine functionalized multiwalled carbon nanotube modified electrode for the determination of hydrogen peroxide. *Carbon* (2007) 1340–1353.
- [31] M. Salavati-Niasari and M. Bazarganipour, Covalent functionalization of multi-wall carbon nanotubes (MWNTs) by nickel(II) Schiff-base complex: Synthesis, characterization and liquid phase oxidation of phenol with hydrogen peroxide. *Appl. Surf. Sci.* 92008) 2963–2970.



- [32] Y.H. Li, C. Xu, C. B. Wei, X. Zhang, M. Zheng, D. Wu and P.M. Ajayan, Self-organized ribbons of aligned carbon nanotubes. *Chem. Mater.* (2002) 483-485.
- [33] A. Koty, M. Sharma, B. Khare and A. Srivastava, Spectrophotometric Determination of Penicillamine with 2,6-Dichlorophenolindophenol in Drug Formulations. *Asian. J. Chem.* (2008) 4239-4248.
- [34] A.J. Bard and L.R. Faulkner, *Electrochemical Methods: Fundamentals and Applications*, 2nd Edition, New York: Wiley (2001).
- [35] A.B. Florou, M.I. Prodromidis, M.I. Karayannis and S.M. Tzouwara-Karayanni, Flow electrochemical determination of ascorbic acid in real samples using a glassy carbon electrode modified with a cellulose acetate film bearing 2,6-dichlorophenol indophenol. *Anal. Chim. Acta* (2000) 113–121.

## کاربرد نانولوله های کربنی عامل دار شده با ۶و۲ دی کلروفنولیندوفنول برای تعیین الکتروکاتالیستی یون های سولفید

علیرضا محدثی\*، سمیه پرورش، زرین اسحاقی، محمدعلی کریمی

بخش شیمی، دانشگاه پیام نور، تهران، ایران

تاریخ دریافت: ۲۴ مرداد ۱۳۹۹ تاریخ پذیرش: ۶ شهریور ۱۳۹۹

### چکیده

یک الکتروود کربن شیشه ای توسط نانولوله های کربنی چند دیواره عامل دار شده با ۶و۲ دی کلروفنولیندوفنول اصلاح گردید. تثبیت این ماده بر روی نانولوله های کربنی توسط اسپکتروسکوپی جذبی UV-vis و FT-IR تایید و به روش ولتامتری چرخه ای اندازه گیری شد. پاسخ الکتروود اصلاح شده دلالت بر پیشرفت فرایند الکتروکاتالیستی، حساسیت و پایداری و تعیین یون های سولفید داشت. ضمن اینکه وابستگی جریان به غلظت سولفید بررسی و گستره خطی ۱,۸ میکرو مولار تا ۲,۵ میلی مولار بدست آمد. حد تشخیص سولفید ۱,۱ میکرومولار و RSD برای سولفید با غلظت های ۱۰ و ۱۰۰ میکرومولار به ترتیب ۱,۸ و ۱,۳ درصد بدست آمد. یون های مزاحم کم تاثیر و یا بدون تاثیر بر روی یون سولفید بودند. روش رای تعیین سولفید در نمونه های آبی بکاربرده شد.

### واژه های کلیدی

۶و۲ دی کلروفنولیندوفنول؛ نانولوله های کربنی؛ الکتروکاتالیست؛ عامل دار کردن.